

The nonlinear response of entangled star polymers to startup of shear flow

Amy K. TezelJames P. OberhauserRichard S. GrahamKamakshi Jagannathan and T. C. B McLeishL. Gary Leal

Citation: [Journal of Rheology](#) **53**, 1193 (2009); doi: 10.1122/1.3160733

View online: <http://dx.doi.org/10.1122/1.3160733>

View Table of Contents: <http://sor.scitation.org/toc/jor/53/5>

Published by the [The Society of Rheology](#)

Articles you may be interested in

[Microscopic theory of linear, entangled polymer chains under rapid deformation including chain stretch and convective constraint release](#)

[Journal of Rheology](#) **47**, 1171 (2003); 10.1122/1.1595099

[Dynamics of entangled linear polymer melts: A molecular-dynamics simulation](#)

[The Journal of Chemical Physics](#) **92**, 5057 (1998); 10.1063/1.458541



**Your future-proof
rheometer.**

MCR 702 TwinDrive™



Get in touch: www.anton-paar.com

The nonlinear response of entangled star polymers to startup of shear flow

Amy K. Tezel^{a)}

*Department of Chemical Engineering, University of California at Santa Barbara,
Santa Barbara, California 93106*

James P. Oberhauser

*Polymer Research and Development, Abbott Vascular, 3635 Peterson Way,
Santa Clara, California 95054*

Richard S. Graham

*School of Mathematical Sciences, University of Nottingham, Nottingham
NG7 2RD, United Kingdom*

Kamakshi Jagannathan and T. C. B McLeish^{b)}

*School of Physics and Astronomy, University of Leeds, Leeds LS2 9JT,
United Kingdom*

L. Gary Leal^{c)}

*Department of Chemical Engineering, University of California at Santa Barbara,
Santa Barbara, California 93106*

(Received 4 February 2009; final revision received 5 June 2009)

Synopsis

We consider the response of entangled four-arm polybutadiene star solutions to steady shear and to startup of steady shear in the nonlinear shear-rate regime. Data are reported both for the shear stress, measured in a cone and plate geometry using a temperature controlled ARES rheometer, and for birefringence measured in a Couette device using two-color birefringence. These data are then compared with predictions from the Mead–Larson–Doi (MLD) and Graham, Likhtman, McLeish and Milner (GLaMM) models for linear chains, but with the reptation mechanism turned off as an “*ad hoc*” means of accounting for the effect of the immobile branch point in these systems. The results for both models are reasonable. However, with the Milner–McLeish model for chain length fluctuations included, the MLD model gives better results at the lowest shear rates where the deep

^{a)}Present address: Allergan, 71 S. Los Carneros, Goleta, CA 93117.

^{b)}Present address: Pro-Vic-Chancellor (Research), Dept. of Physics, Durham University, Durham SH1 3UP, United Kingdom.

^{c)}Author to whom correspondence should be addressed; electronic mail: lgl@engineering.ucsb.edu

retractions of the arms are a significant contributor to chain relaxation. On the other hand, the local implementation of convective constraint release (CCR) in the GLaMM model gives better predictions for higher shear rates between the inverse reptation and inverse Rouse times, where the CCR mechanism largely obviates any contribution of the deep arm retractions to the relaxation process. © 2009 *The Society of Rheology*. [DOI: 10.1122/1.3160733]

I. INTRODUCTION

Star polymers are useful in their own right because of their large zero-shear viscosity and strong shear thinning behavior. In addition, stars are often used as rheological modifiers, added to linear polymers to increase viscosity. From a more fundamental point of view, however, star polymers have been the subject of many studies, especially in the linear viscoelastic regime, because they are the simplest example of a branched polymer, having N arms and a single branch point. Indeed, previous studies of entangled star polymers have looked at their terminal relaxation time [Bero and Roland (1996)], diffusion coefficient [Shull *et al.* (1990)], zero-shear viscosity and dynamic moduli [Raju *et al.* (1981)], rheo-dielectric behavior [Watanabe *et al.* (2002)], steady state shear and extensional properties [Tezel *et al.* (2005); Ye and Sridhar (2001)], and their nonlinear rheological behavior [Tezel *et al.* (2005); Ye and Sridhar (2001); Menezes and Graessley (1982); Fetters *et al.* (1993); Vega and Milner (2007)].

In the linear viscoelastic regime, the relaxation spectrum of a star polymer is very different from that of a linear chain of the same span molecular weight. This is because the relaxation mode known as reptation is essentially prohibited by the immobility of the branch point. This causes relaxation of flow-induced orientation of the arms to be dominated by contour length fluctuations (CLFs), coupled with constraint release (CR). The latter has been successfully modeled for this system via the dynamic dilution approximation. As a consequence of the dominance of CLF, the longest relaxation times increase exponentially with the molecular weight (MW) of the arms, and the linear rheology is fundamentally different to linear polymers. In fact, these differences are well understood. A comprehensive theoretical framework was developed by Milner and McLeish (1997) that is very successful in predicting the linear viscoelastic behavior of both classes of polymers.

In the nonlinear regime, the external flow modifies the polymer relaxation, and convective constraint release (CCR) plays an important role for both star and linear polymers [Tezel *et al.* (2005); Milner *et al.* (2001)]. This mechanism describes relaxation due to the release of entanglements caused by relative motions of polymer chains, due primarily to the rapid retraction of chains from the affine deformation with the flow. The corresponding CR rate is proportional to the shear rate at rates that exceed the inverse terminal relaxation time. This mechanism is expected to be very similar for linear and star polymers; hence, at shear rates where this is the dominant relaxation mechanism, their nonlinear rheological behavior is also expected to be very similar. In fact, Tezel *et al.* (2005) showed in an earlier study of steady shear flows (albeit, only for a single polymer) that the exact same model of CCR quantitatively describes the relaxation process for both linear and star polymers. Thus, the *steady* shear rheology in the *nonlinear* regime looks very similar for linear and star-branched polymers.

In the present work, we provide some additional data to corroborate the equivalence of CCR for linear chains and star arms in steady shear flow. We also provide data for the transient behavior during the startup of steady shear flow. These data again show that the nonlinear rheological response of linear and star-branched polymers is very similar.

This suggests the interesting hypothesis that the transient response of star polymers might be predicted using nonlinear models derived for linear polymers, with the only

TABLE I. Properties of studied star polymer solutions.

Polymer	M_n (g/mol)	PDI	wt %	G_N^0 (Pa)	Z	τ_e (s)	τ_{longest} (s)
Star 2	570000	1.13	13	21125	10	6.5E-05	20
Star 3	330000	1.034	22	60500	9.8	2.0E-05	6.1
Star 4	330000	1.034	15	25125	6.7	5.8E-05	1
Star 5	530000	1.00	14	25000	10	5.8E-05	15.9
Star 6	530000	1.00	12	18000	8.6	5.8E-05	4.84
Linear 1	615000	1.025	6	1762	7.8	3.4E-03	2.68

change being to simply “turn-off” the reptation mechanism. In our previous study of steady flows [Tezel *et al.* (2005)], we derived a very simple model based on the direct application of a model for CCR in linear chain polymers. Unfortunately, the assumptions underlying this model break down in transient flows. On the other hand, at least two general nonlinear models have been proposed for linear chains that include CCR, namely, the Mead–Larson–Doi (MLD), model due to Mead *et al.* (1998), and the more recent Graham, Likhtman, McLeish and Milner (GLaMM) model of Graham *et al.* (2003). In the present study, we compare both steady and transient data to predictions from these models, which we shall refer to as MLD-R and GLaMM-R, the R being included to remind the reader that the reptation mechanism is turned off in the comparisons with stars.

Recent experimental studies of star polymers in the nonlinear regime have been limited primarily to measurements of steady state behavior as a function of shear rate [Tezel *et al.* (2005)] and the step-strain relaxation modulus $G(t, \gamma)$ [Ye and Sridhar (2001); Vega and Milner (2007)]. The best-known early study by Menezes and Graessley (1982) of entangled stars also presented measurements of the steady state shear stress and first normal stress difference, along with measurements of the stresses during startup of shear flow, measured on a Weissenberg rheogoniometer. This was contrasted with similar experimental measurements for a range of linear polymers. Their results for the star solution will be discussed later in this paper.

II. EXPERIMENTAL DETAILS

Symmetric four-arm polybutadiene stars were made using anionic synthetic techniques described in our earlier paper [Tezel *et al.* (2005)]. The resulting stars were put into solution at concentrations ranging from 12 to 22 wt % in low molecular weight polybutadiene ($M_n=1800$ g/mol) using tetrahydrofuran as a co-solvent. The co-solvent was evaporated by slowly stirring the solution under vacuum until a constant weight was maintained. For comparison, a linear polybutadiene was also synthesized anionically. The linear chain was put into solution in the same solvent at 6 wt %.

The linear viscoelastic behavior of each solution was characterized by performing frequency sweeps on a strain controlled ARES rheometer over a range of temperatures. The resulting moduli were shifted using time-temperature superposition to a reference temperature of 22 °C. The properties, including the plateau modulus G_N^0 , the intrinsic relaxation time of an entanglement segment τ_e , the concentration in solution wt %, the number of entanglements per chain Z , the polydispersity index PDI, and the longest relaxation time τ_{longest} , are listed in Table I for the six polymer solutions that we use in

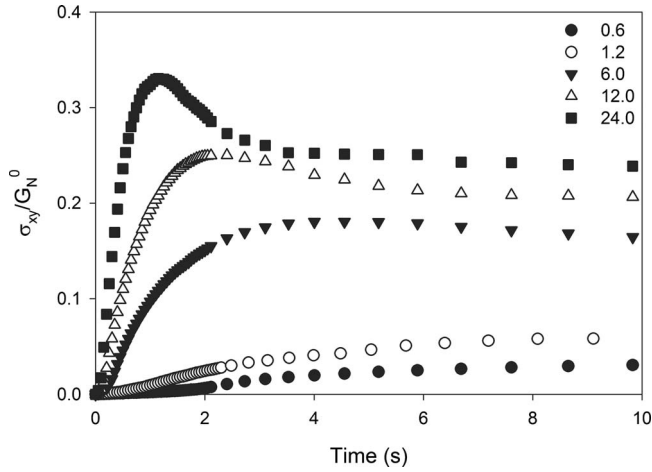


FIG. 1. The response of star 2 to the startup of shear flow at different shear rates. The shear rates are expressed in terms of the Weissenberg number Wi , which is defined as the shear rate multiplied by the longest relaxation time of the star (20 s).

this work. A thorough discussion of how these parameters were determined is presented in the Ph.D. thesis of [Tezel \(2005\)](#), including the evidence that a dilution factor $\alpha=1$ provides a “best fit” of the data for these star polymers.

In order to measure the response of these solutions to the startup of shear flow, two experimental methods were used. A temperature controlled ARES rheometer using a 50 mm cone and plate (cone angle 0.04 rad) directly measured the shear stress upon the application of a given shear rate. This rheometer is not equipped to directly measure the first normal stress difference. However, such a fixture is available from the manufacturer and would be useful for further studies. All transient rheological measurements were carried out at room temperature, 22 °C. In order to obtain a more complete description of the stress tensor as a function of time and shear rate, experiments were also carried out in a Couette shear cell using the two-color flow birefringence apparatus described in detail elsewhere [[Chow and Fuller \(1984\)](#); [Geffroy and Leal \(1990, Geffroy and Leal 1992\)](#)]. This apparatus allows for the nearly instantaneous application of a prescribed shear rate. We measure the birefringence Δn and the angle between the principle axis of the refractive index tensor and the flow direction, which we term the “orientation angle” χ . These rheo-optical quantities can be converted to a shear stress and first normal stress difference using the stress-optical rule, with the literature value of the stress-optical coefficient, namely, $C=2.2 \times 10^{-9} \text{ m}^2/\text{N}$ [[Macosko \(1994\)](#)].

The two experiments have advantages and disadvantages. The mechanical rheometer gives measurements with very little noise but can only measure shear stress. Also, the maximum torque that can be measured limits the shear-rate range of the experiments, although in the future this problem could be lessened by using smaller cone and plate fixtures. The optical rheometer has the advantage of being able to infer both the shear stress and first normal stress difference.

III. EXPERIMENTAL RESULTS FOR STARTUP OF STEADY SHEAR

The transient shear stress response of the different star solutions listed in [Table I](#) was measured at various shear rates. The results for star 2 are presented in [Fig. 1](#), showing the shear stress as a function of time for different values of the Wi number, ranging from 0.6

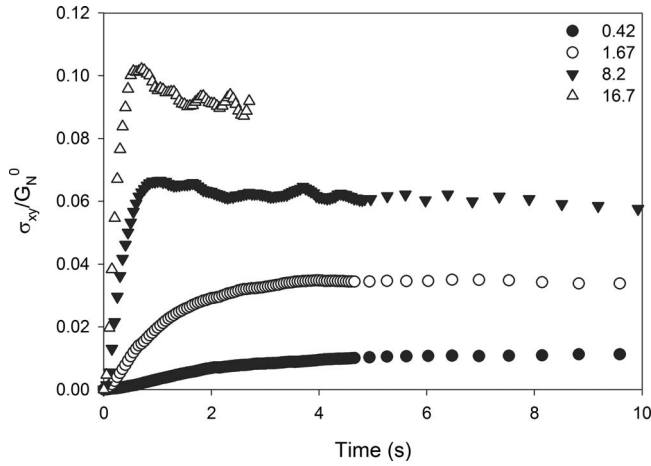


FIG. 2. The response of star 3 to the startup of shear flow at different Wi . The longest relaxation time for this star is 6.1 s.

up to 24. The Weissenberg number is the shear rate scaled with respect to the longest relaxation times in Table I, namely, $Wi \equiv \dot{\gamma}\tau_{\text{longest}}$. The most notable feature is the onset of a shear stress overshoot above Wi of the order one. The width of the overshoot (when plotted versus time) decreases with increasing Wi , while the magnitude of the overshoot increases with increasing Wi . Throughout this study, all shear rates are in the range $\dot{\gamma}\tau_R \leq O(1)$ so chain stretching is not expected.

Similar results are shown for stars 3, 4, and 6 in Figs. 2–4. These results differ in detail due to their different molecular weights and concentrations in solution; however, the general behavior is similar to star 2. The onset of the shear stress overshoot occurs consistently for $Wi \geq 2$. As expected, based upon the discussion in Sec. I, literature results for similar experiments on linear polymers show the same qualitative behavior: a shear stress overshoot consistently appears at shear rates greater than the inverse of the longest relaxation time [[Menezes and Graessley \(1982\)](#); [Sanchez-Reyes and Archer](#)

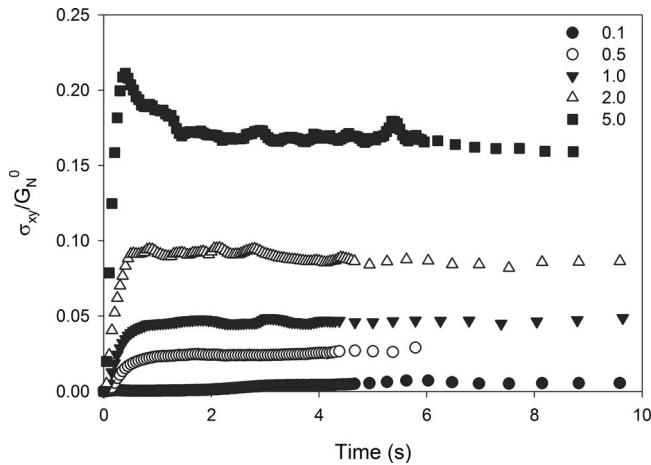


FIG. 3. The response of star 4 to the startup of shear flow at different Wi . The longest relaxation time for this star is 1 s.

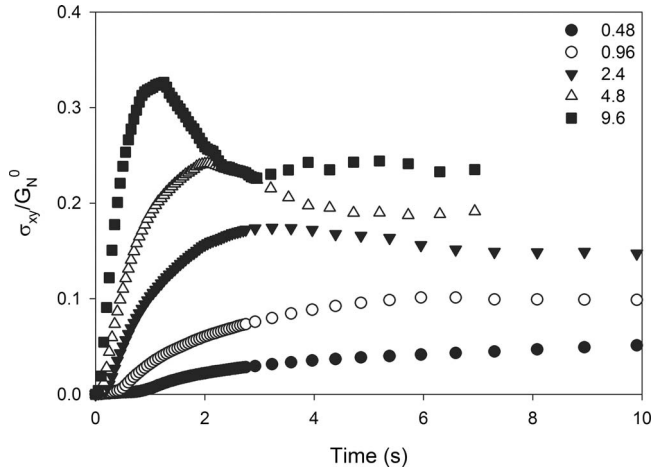


FIG. 4. The response of star 6 to the startup of shear flow at different Wi . The longest relaxation time for this star is 4.8 s.

(2003); Islam and Archer (2001)]. The one other study by Menezes and Graessley (1982) that presented startup shear stress data for a solution of stars does not provide a longest relaxation time. However, an approximate fit of the provided linear viscoelastic data leads to a longest relaxation time of 0.3 s. In that study, overshoots were seen at shear rates of 10.8 s^{-1} and greater but not at shear rates of 5.4 s^{-1} and less. This corresponds to overshoot at approximately $Wi=3.2$, with no overshoot at $Wi=1.6$, which is in qualitative agreement with the present results.

The other notable feature of these four sets of results is that the shear stress maximum occurs at a strain of the order one in each instance, consistent with Menezes and Graessley's (1982) previous findings for stars. Comparable results are also seen for linear polymers. For example, Menezes and Graessley (1982) and Inoue *et al.* (2004) reported shear stress maxima at strains of 2, and Pearson *et al.* (1989) observed shear stress maxima at strains of 2.3. Another study of linear polymers due to Chai *et al.* (1999) noted that for intermediate Wi (shear rates above the inverse of the longest relaxation time, but less than the inverse Rouse time), the shear stress maximum occurs at a constant strain. In this flow regime, the overshoot is a geometric effect, being a consequence of instantaneous chain retraction and essentially affine rotation of the tubes. This means that the strain at peak stress is not strongly dependent on molecular weight, as observed experimentally. CCR reduces the effective strain experienced by the chain and, eventually, leads to its steady state value. In contrast, Chai *et al.* (1999) found that overshoots at higher shear rates (exceeding the inverse Rouse time) occur at constant time rather than constant strain and are associated with polymer stretch.

In order to obtain a more complete picture of the response of the entangled star solutions to startup of shear, star 2 was also studied using the two-color flow birefringence apparatus. Rather than measuring one variable as a function of strain or time, two were measured: the retardance, which is proportional to the birefringence, and the orientation angle. Some mechanical rheometers are capable of measuring both shear stress and first normal stress difference simultaneously; however, transducer compliance effects can complicate normal stress measurements, especially in transient flows [cf. Brown *et al.* (1995)]. Rheo-optical experiments have the advantage of being noninvasive. The mea-

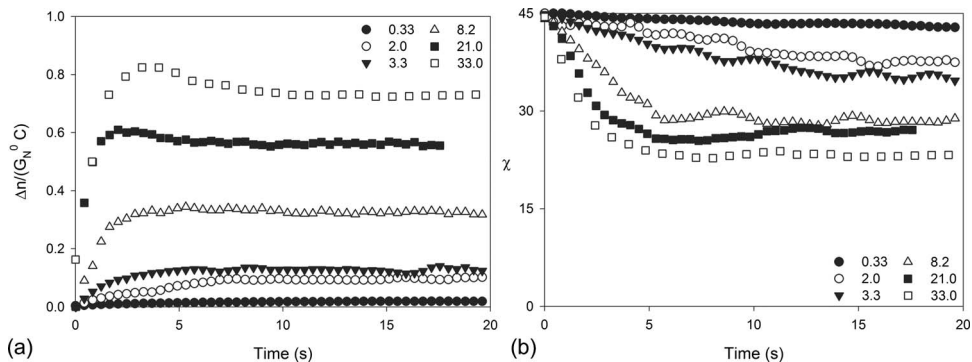


FIG. 5. Transient rheo-optical data for startup of shear for star 2 at several Wi . (a) Birefringence; (b) orientation angle.

sured birefringence and orientation angle can be converted to shear stress and first normal stress difference by the use of the stress-optical rule provided $\dot{\gamma}\tau_R \leq O(1)$ as in this study.

The birefringence is defined as the difference between the parallel and perpendicular components of the index of refraction tensor. Increased birefringence means an increase in the degree of optical anisotropy of the system as chain segments become more aligned with one another. As defined previously, the orientation angle is the angle between the principle axis of the refractive index tensor and the flow direction. A nearly isotropic system will have an orientation angle of 45° corresponding to the angle of the principle strain-rate axis. As the shear rate is increased, the orientation angle rotates toward 0° , which corresponds to complete alignment of the polymer chain with the flow direction.

Transient birefringence and orientation angle results for star 2 are presented in Fig. 5. The birefringence is non-dimensionalized by the product of the plateau modulus and the stress-optical coefficient. This commonly used scaling of the birefringence has a physical interpretation [Oberhauser *et al.* (1998); Oberhauser (2001)]. When $\Delta n / G_N^0 C \sim O(1)$, there is full alignment of the primitive chain with the flow, but no chain stretch. Higher values of the non-dimensionalized birefringence indicate chain stretch. However, the shear rates in our experiments are less than the inverse Rouse time so chain stretching is not expected to occur. Our observation that $\Delta n / G_N^0 C < O(1)$ is consistent with this.

The steady state birefringence increases with Wi as expected, meaning that the flow causes chains to preferentially align with one another. For higher Wi , there are visible overshoots in birefringence. The steady state orientation angle decreases with increasing Wi once the time scale of the flow becomes faster than the longest relaxation time. At these shear rates, the tube is deformed at a rate that exceeds its ability to relax and it is aligned toward the flow. The transient decrease in the orientation angle with time does not show the distinct undershoot seen in linear chains when the Wi based on the Rouse relaxation time is greater than one [Chai *et al.* (1999)], further confirming the absence of the chain stretch.

Finally, we also examined the linear polymer, “linear 1” listed in Table I, for startup of shear flow using two-color flow birefringence. The results are shown in Fig. 6. The results for this linear chain are shown for qualitative comparison, as the number of entanglements, the plateau modulus, and the relaxation times are different. The birefringence increases monotonically with increasing Wi as was the case for star 2, with higher shear rates leading to an overshoot in birefringence. The results for the orientation angle as a function of time for different Wi show that the steady state orientation angle de-

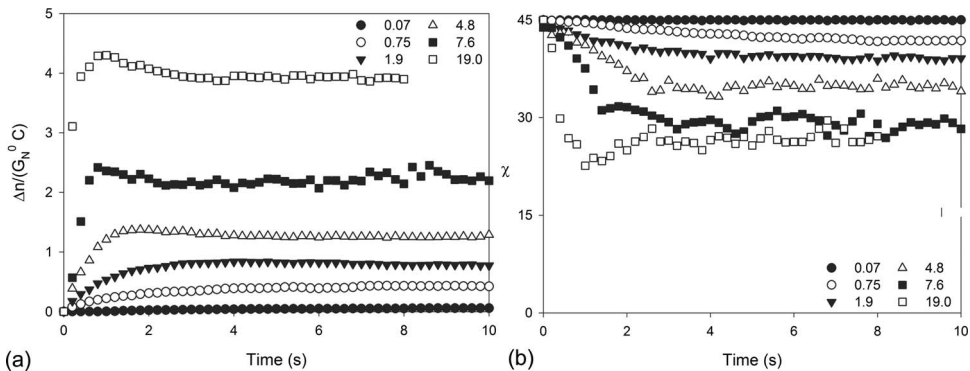


FIG. 6. Transient rheo-optical data for startup of shear for linear 1 at several Wi . (a) Birefringence; (b) orientation angle.

creases with increasing Wi , as expected. However, there is an obvious orientation angle undershoot for $Wi=19$. If the Wi was defined in terms of the Rouse time rather than the longest relaxation time, the largest value for the linear chain would be $Wi_R \equiv \dot{\gamma}\tau_R = 3.2$. [Chai *et al.* \(1999\)](#) observed that orientation angle undershoots occur for γ , indicating the presence of chain stretch. The orientation angle undershoot corresponds to a maximum in chain length, before the stretch is relaxed and the chain (tube) comes to a steady state length. The maximum Wi_R for star 2 was less than 1, so no orientation angle undershoot was expected or found.

IV. COMPARISONS WITH THEORETICAL MODELS

We now address the question of whether the results of the preceding section can be reproduced by adapting existing nonlinear models for linear polymers. We adopt the simplest possible assumption, namely, that all aspects of the nonlinear model are preserved when applied to star arms except that relaxation by reptation is turned off. We consider two models, namely, one based on the model of [Mead *et al.* \(1998\)](#) that we have denoted as MLD-R and the other based on the work of [Graham *et al.* \(2003\)](#) that we have denoted as GLaMM-R. Both contain a model for CCR, and both have previously been compared with the experimental data for linear chains [[Bhattacharjee *et al.* \(2002\)](#); [Patamaprom and Larson \(2001\)](#); [Ye *et al.* \(2003\)](#); [Isaki \(2003\)](#); [Schweizer *et al.* \(2004\)](#); [Auhl *et al.* \(2008\)](#)]. For linear chains, both models provide reasonable predictions in steady shear. However, in the startup of shear, the MLD model tends to under-predict the magnitude of the shear stress overshoot, while the GLaMM model slightly over-predicts the same quantity at very high rates.

The details of the theoretical models have both been described in detail in the original papers [[Mead *et al.* \(1998\)](#); [Graham *et al.* \(2003\)](#)]. A summary of these models and the changes introduced to model stars are shown in the Appendix. Apart from the deletion of reptation, the MLD-R model used here contains only one significant change from the original MLD publication. The form of the CLF component of the equation differs from the Doi-Kuzuu form used in the original MLD model and is instead based on the most recent and successful models for CLF coming from [Milner and McLeish \(1998\)](#), with prefactors later corrected by [Likhtman \[\[Likhtman and McLeish \\(2002\\)\]\(#\); \[McLeish \\(2002\\)\]\(#\)\]](#). This version of CLF has dynamic dilution already built-in, meaning that the chain ends are allowed to fluctuate while simultaneously the effective tube radius in which they are fluctuating grows due to the release of entanglements by relaxed segments of neighboring

chains. The GLaMM-R model is identical to the published GLaMM model, except reptation is suppressed by modifying the diffusive function that controls both reptation and CLF in this model [Eq. (23) of [Graham *et al.* \(2003\)](#)]. For stars, the $1/Z$ region of this function, which corresponds to reptation, is set to zero. All other features of the model remain the same. This modification will correctly account for the early time shallow fluctuations of the star arms since these are present in linear polymers. However, the deep activated fluctuations may not be accurately captured by this modification and so some deviation in linear response where these deep fluctuations dominate is expected.

Both the MLD and the GLaMM models assume that chain deformation does not change the cross-section of the tube. That is, the tube diameter remains fixed under flow. This initially appears to contradict the ideas of dynamic dilution, in which the tube diameter grows in time. However, these two approaches are, in fact, self-consistent. The tube diameter is the distance a chain can move before it feels the effect of the surrounding chains and this does not change during linear flow, for which dynamic dilution was originally derived. However, dynamic dilution realizes that for deep segments, which relax very slowly, most of the surrounding chains will relax many times over during the time it takes for the deep segment to relax. Thus, a deep segment feels only constraints from other slow moving segments. This means that the *effective* tube diameter felt by a deep segment is a diluted version of the underlying tube diameter. Thus, the effective tube diameter grows with time following a small step strain even though the underlying tube diameter is fixed. The MLD-R and GLaMM-R models implement this arm retraction process by assigning an effective diffusion constant for each chain section, chosen to give a relaxation time consistent with dynamic dilution in linear response. They also both assume that flow does not have a strong effect on the confining potential experienced by a chain due to its neighbors. Thus, the physics of dynamic dilution does not change under flow, which is consistent with the assumption that the underlying tube diameter does not change with flow. This constant tube diameter assumption also affects the other relaxation processes, especially CR, although its direct effects are most pronounced in stretching flows, which are not studied in this work.

The MLD and GLaMM models do, however, differ in a number of ways. The main focus for the present work is the fundamentally different way that they incorporate CCR since this is primarily responsible for the differences in their predictions for star polymers in the present flows. In the MLD model, CR is implemented as a modification to the tube survival probability function. Thus, CCR effectively augments relaxation via reptation and chain length fluctuations, effectively reducing the overall chain relaxation time, and thus reducing the size of any stress overshoots. The GLaMM model implements the relaxation mechanisms of reptation, CLF, CR (both thermal and convective), and chain retraction at the length scale of the tube diameter. In contrast to MLD, in the GLaMM model, CR is recognized as a completely distinct relaxation mechanism to reptation and CLF, which arises from lateral hops of the tube acting at the length scale of the tube diameter. Hence, the GLaMM model implements CR as local hops of the tube, leading to Rouse-like motion of the tube itself.

The difference between the two approaches to modeling CCR, hence between the MLD-R and GLaMM-R models, is likely to be particularly important in star polymers. In stars, CCR is expected to play a more pronounced role because of the wide separation of stretch and orientation time scales. Furthermore, CCR is envisioned as acting evenly along the stars arms, so it is expected to smooth out the strong exponential dependence of the relaxation time on the position along the arm. This effect is captured in the *locally* correct GLaMM implementation of CCR. In contrast, the reduction in the overall chain

relaxation times inherent in the approach of the MLD model will preserve this exponential separation of relaxation times along the arm even under strong flow conditions.¹

A. Steady shear behavior

We begin by considering the prediction of star behavior in a steady shear flow. We showed in our previous study [Tezel *et al.* (2005)] for a single lower molecular weight four-arm star that the shear stress and the normal stress (thus also the birefringence and orientation angle) could be predicted very accurately via a very simple superposition model, in which it was assumed that the chain configuration for the outer portion of each arm was determined by the linear viscoelastic relaxation mechanism for a linear polymer but with reptation suppressed (the outer portion being defined as the region where the linear viscoelastic relaxation time is shorter than the inverse of the shear rate), whereas the chain configuration for the remaining portion of the arms was dominated by CCR.

Unfortunately, there is no way of applying this simple idea to the transient data for start-up flow. Hence, for start-up flows, we are forced to consider the full nonlinear models discussed above. Although there is no assumption of a simple superposition principle built explicitly into these models, they should be able to reproduce the steady shear data since the full model should reflect a comparable separation of relaxation mechanisms as a function of position along the star arms. The main difference is that the transition from linear viscoelastic relaxation mechanism to CCR is not as abrupt as it was assumed to be in the simple superposition model. Indeed, steady state is reproduced by both models, essential through the same relaxation processes as in the simple superposition model.

Hence, as a first test of the basic idea of using models for linear chains to model the dynamics of stars, we initially made a comparison between the predictions of the MLD-R and GLaMM-R models and birefringence data for a steady shear flow. In addition to the data for the four-arm star from our previous study, we also obtained steady shear data for the entire set of star polymers listed in Table I. In particular, the steady state birefringence and orientation angle were measured as a function of Wi using two-color flow birefringence, as described by Tezel *et al.* (2005) and Tezel (2005). The stress-optical rule was then used to convert these results into shear stress and first normal stress difference. These experimental measurements, as well as the predictions from the MLD-R and GLaMM-R models, are shown in Figs. 7–11.

Both the MLD-R and GLaMM-R models show reasonable qualitative agreement with the majority of the data for the larger shear rates, though it could be argued that the GLaMM-R model does a slightly better job in this regime. Both models, but especially the GLaMM-R model, tend to show deviations at lower shear rates corresponding to Wi of the order one or less. However, at least with the parameter values used here, the MLD model provides somewhat better agreement with the steady state data in this regime of low shear rates. It should be noted that the results shown in Figs. 7–11 are plotted in a log-log format, and this tends to minimize some significant quantitative deviations between both the model predictions and the comparisons with the data.

¹In the GLaMM model, the effectiveness of CCR after any chain stretch is also decreased due to the assumption of a fixed persistence length. The physical reason is that the number of tube segments for any fixed fraction of the chain is increased, hence, requiring more “tube hops” for complete relaxation. This reduces the effect of CCR and, hence, tends to preserve the magnitude of overshoots. The MLD model (and thus MLD-R) does not incorporate this reduction in the effectiveness of CCR with chain stretch, and, in the range $\dot{\gamma}\tau_R \geq O(1)$, it is likely that this is an additional reason that it produces significantly weaker overshoots than the GLaMM model for startup flow for linear chains.

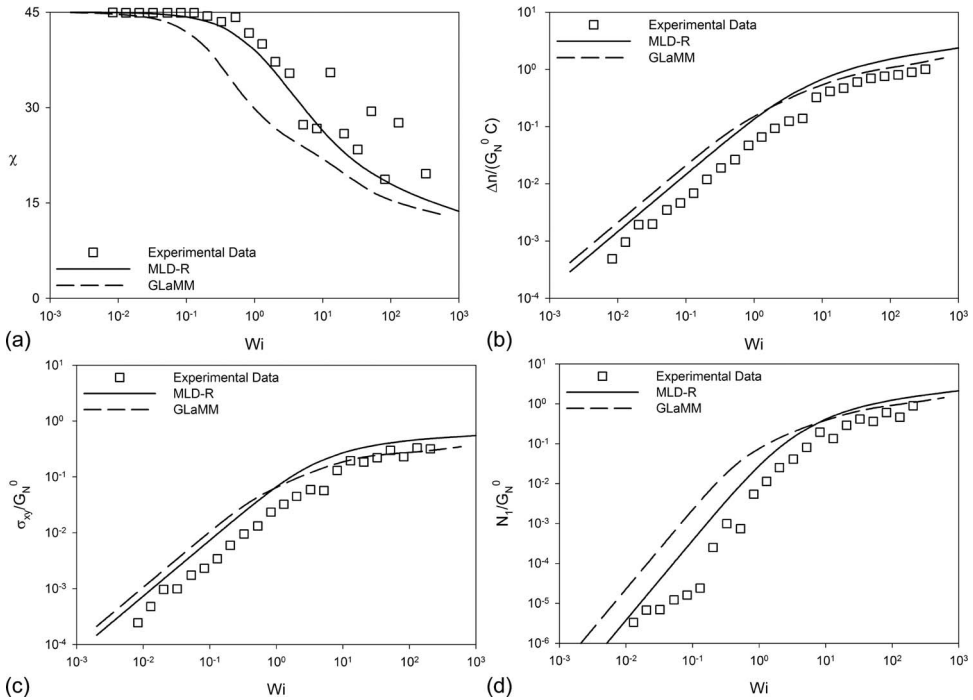


FIG. 7. [(a)–(d)] Steady state comparisons between experimental measurements and the MLD-R and GLaMM-R models for star 2. The plots show birefringence, orientation angle, shear stress, and first normal stress difference plotted as a function of Wi . The shear stress and first normal stress “data” are calculated from the birefringence and orientation angle data using the stress-optical law and a stress-optical coefficient $C = 2.2 \times 10^{-9} \text{ m}^2/\text{N}$ (Macosko, 1994).

The comparisons shown in Figs. 7–11 allow for no adjustable parameters and use parameters that are available from the literature or from our linear viscoelastic measurements. In particular, no attempt was made to adjust the parameters to optimize the fits of the two models to the data. The values of the parameters do depend on the dilution parameter α , which is assumed to have a value of 1. Different values of the dilution parameter will lead to dramatically different predictions for the model parameters G_N^0 , M_e , and τ_e , as they scale with concentration to the α , $\alpha+1$, and 2α powers, respectively. There has been much literature discussion of the correct value of the dilution parameter. Common choices are $\alpha=1$, which defines an entanglement as a binary event, or $\alpha=4/3$, which indicates that an entanglement is made up of interactions between more than two neighboring chains. A thorough discussion of why $\alpha=1$ was selected for this work is given by Tezel (2005).

The qualitative agreement between the measured values and those predicted by the GLaMM-R and MLD-R models using no adjustable parameters further confirms the conclusion from our earlier study [Tezel *et al.* (2005)] that it is reasonable to model the dynamics of star arms in the same way as linear chains but with reptation removed. We emphasize here that τ_e was adjusted to match the linear viscoelastic data, as in Likhtman and McLeish (2002), but that no fitting was used when comparing the MLD-R and GLaMM-R models to our nonlinear flow data. Across all of these figures, the MLD model does a better job of predicting the lower shear rate behavior because it reproduces the behavior of the Milner–McLeish model more closely than the GLaMM-R model

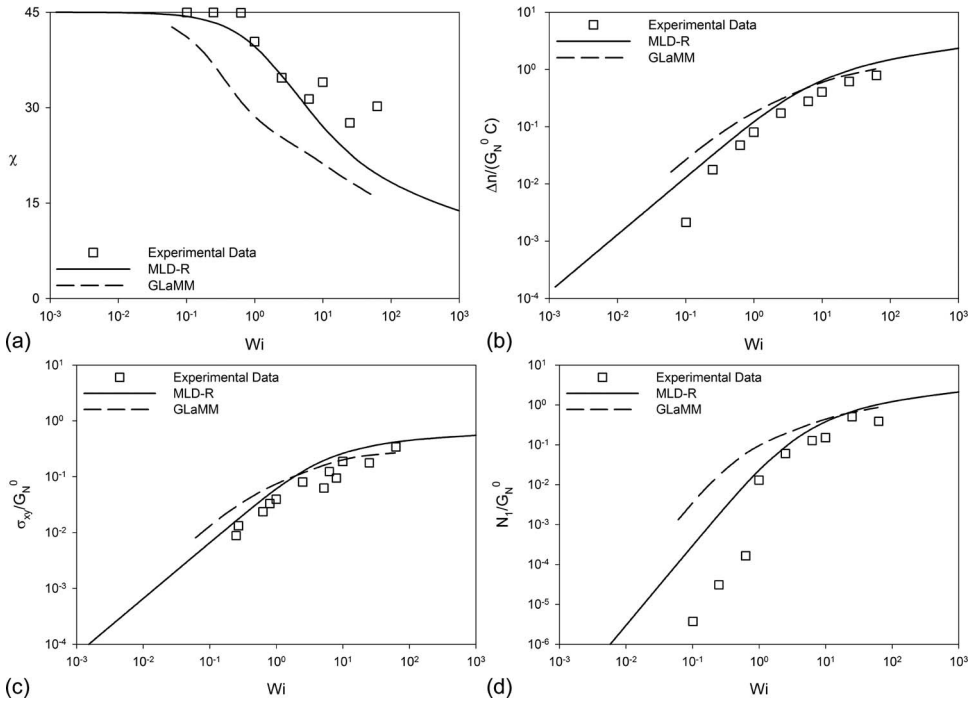


FIG. 8. (a)–(d) Steady state comparisons between experimental measurements and the MLD-R and GLaMM-R models for star 3. The plots show birefringence, orientation angle, shear stress, and first normal stress difference plotted as a function of Wi . The shear stress and first normal stress data are calculated from the birefringence and orientation angle data using the stress-optical law and a stress-optical coefficient $C=2.2 \times 10^{-9} \text{ m}^2/\text{N}$ (Macosko, 1994).

does. In particular, the MLD model accurately accounts for deep fluctuations through the CLF expression from the Milner–McLeish model. However, at higher shear rates the GLaMM model captures the experimental data better than the MLD model because here CCR dominates over deep fluctuations and so the GLaMM model’s superior implementation of CCR proves to be more accurate. We conclude that an accurate implementation of Milner–McLeish deep fluctuations combined with the GLaMM model’s CCR implementation would be expected to account for the full range of flow rates.

B. Transient start-up behavior

A more challenging test of the MLD-R and the GLaMM-R models’ approach to star polymers is provided by transient start-up flow data. The transient computations were made using the same parameters that were used for the steady state simulations.

The first comparison is with the startup of shear measurements from star 6. This star was chosen because the transient data have distinct features, such as curves for three shear rates that exhibit shear stress overshoots. The same comparisons could easily be made for each of the other stars. In this case, only the shear stresses are compared. Figure 12 shows the measured and predicted values of the shear stress as a function of time for five different shear rates. The Wi associated with these shear rates range from 0.48 to 9.6. The data and predictions for the two models can be identified by noting that there are five curves (or data sets), with the shear stress increasing monotonically with Wi starting from

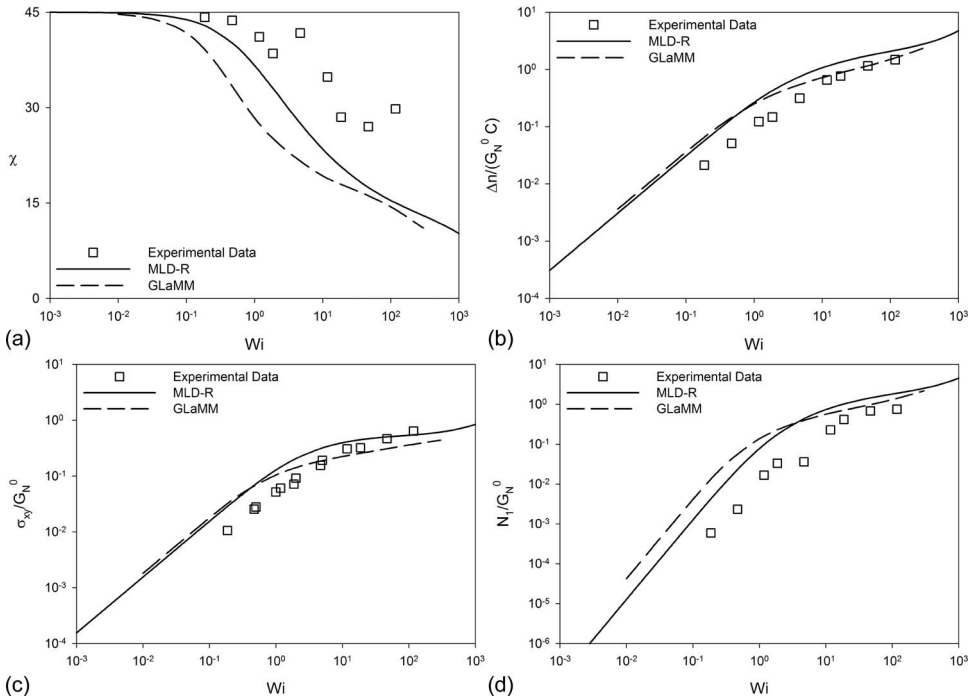


FIG. 9. (a)–(d) Steady state comparisons between experimental measurements and the MLD-R and GLaMM-R models for star 4. The plots show birefringence, orientation angle, shear stress, and first normal stress difference plotted as a function of Wi . The shear stress and first normal stress data are calculated from the birefringence and orientation angle data using the stress-optical law and a stress-optical coefficient $C=2.2 \times 10^{-9} \text{ m}^2/\text{N}$ (Macosko, 1994).

the lowermost curve. Note that in this particular case, the steady state values are better predicted by the GLaMM-R model, whereas the MLD-R theory over-predicts the steady shear stress, especially at the highest two values of Wi .

Both models correctly predict the qualitative features of the transient behavior, including an overshoot in shear stress for $Wi > O(1)$ at strains around 2. The main quantitative difference is that the MLD-R model under-predicts the magnitude of the overshoot in shear stress. For linear chains, Pattamaprom and Larson (2001) previously demonstrated that the MLD model leads to a strong under-prediction of the magnitude of the shear stress overshoot. For shear rates such that $\dot{\gamma}\tau_R \leq O(1)$, the comparison with GLaMM-R suggests that the under-prediction of the overshoots can be attributed to the fact that the CCR is not implemented on a local level in the MLD model.

A more complete test of the GLaMM-R and MLD-R models involves comparing with more than one quantity. In this more rigorous comparison, model predictions were compared with the rheo-optical measurements on star 2 in the startup of shear flow, over a range of shear rates.

Figure 13 shows birefringence plotted as a function of time for different Wi . The experimental results for star 2 are the same as those previously presented in Fig. 5. The main differences between the two models are that the MLD model produces a greater over-prediction of the steady state magnitude of the birefringence and an under-prediction of the magnitude of the birefringence overshoot. Both models over-predict the reduction in the steady state orientation angle, though, in this instance, the MLD model is some-

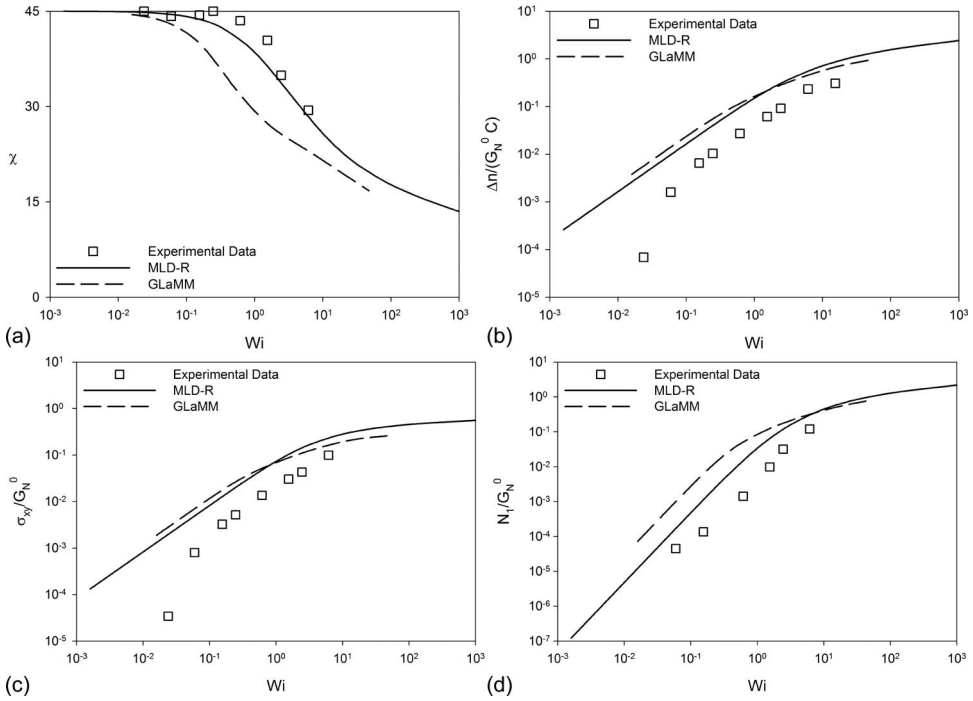


FIG. 10. (a)–(d) Steady state comparisons between experimental measurements and the MLD-R and GLaMM-R models for star 5. The plots show birefringence, orientation angle, shear stress, and first normal stress difference plotted as a function of Wi . The shear stress and first normal stress data are calculated from the birefringence and orientation angle data using the stress-optical law and a stress-optical coefficient $C=2.2 \times 10^{-9} \text{ m}^2/\text{N}$ (Macosko, 1994).

what better. Since the birefringence and shear stress are related, an under-prediction of the birefringence overshoot by the model implies a simultaneous under-prediction of the shear stress overshoot. The other less obvious difference is the time at which steady state is achieved. The measured time to reach the steady state orientation angle is longer than predicted by either model.

The same results are re-expressed as shear stress and first normal stress difference in Fig. 14. The shear stress comparisons are qualitatively similar to those for star 6. The steady state shear stress values are over-predicted by MLD-R, while the magnitude of the overshoot is under-predicted. The predicted first normal stress difference N_1 is closer to the data especially at the highest shear rates. It must be noted that these normal stress values were not measured directly but were inferred from the birefringence data via the stress-optical law, but this is expected to be a reliable approach in the range of parameters considered here. Nevertheless, it would be valuable to obtain normal stress data directly and make another comparison with these models.

In summary, a consistent picture emerges from the comparison with transient data: at higher shear-rates CCR and shallow arm fluctuations dominate and so the GLaMM-R model's local implementation of CCR describes more accurately our experiments than the MLD model's approach, in which CCR speeds up the arm diffusion. In this moder-

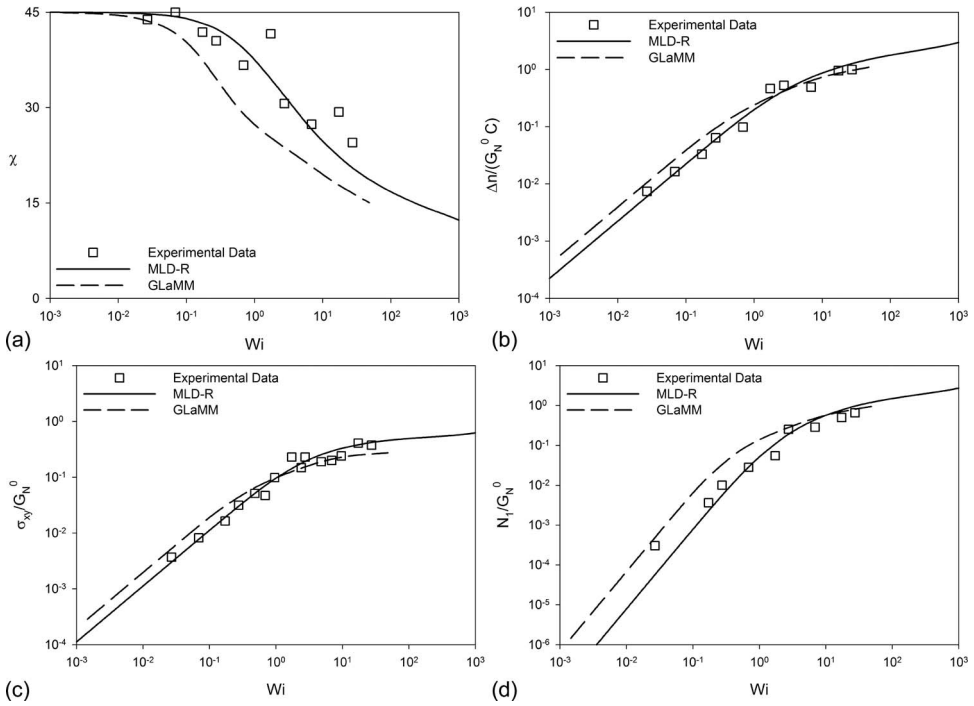


FIG. 11. (a)–(d) Steady state comparisons between experimental measurements and the MLD-R and GLaMM-R models for star 6. The plots show birefringence, orientation angle, shear stress, and first normal stress difference plotted as a function of Wi . The shear stress and first normal stress data are calculated from the birefringence and orientation angle data using the stress-optical law and a stress-optical coefficient $C=2.2 \times 10^{-9} \text{ m}^2/\text{N}$ (Macosko, 1994).

ately non-linear flow rate regime, in which CCR becomes a faster relaxation mechanism than deep fluctuations for arm segments close to the branch point, we would expect the transient response of linear polymers and stars with a matched span molecular weight to be quantitatively very similar.

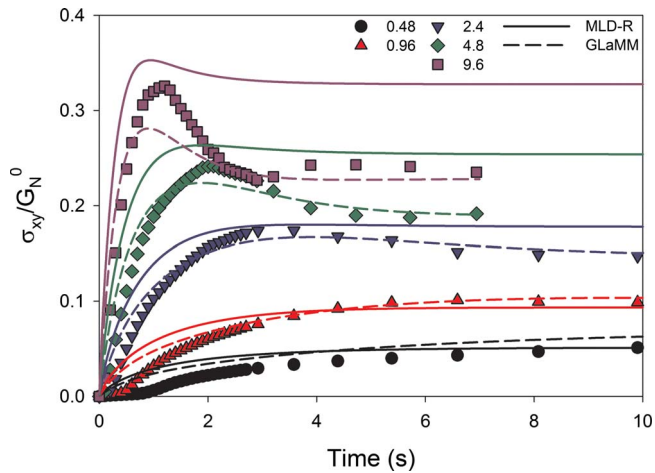


FIG. 12. A comparison of MLD-R and GLaMM-R predictions with data for startup of steady shear flow for star 6 at several different Wi .

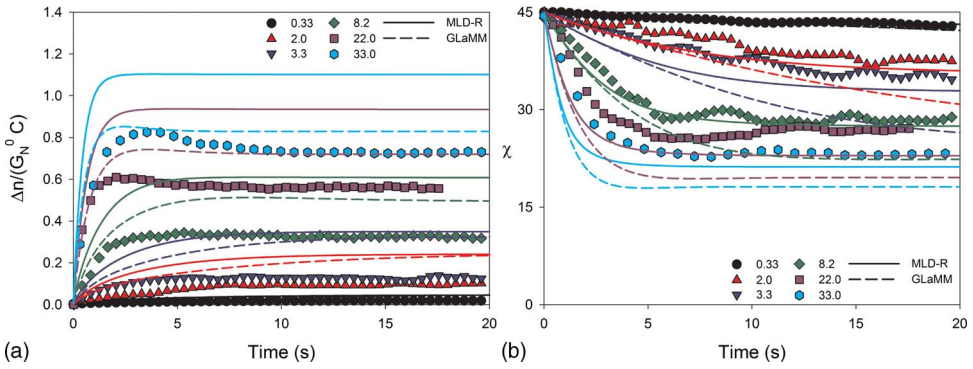


FIG. 13. (a) and (b) A comparison of MLD-R and GLaMM-R predictions with transient rheo-optical data for startup of steady shear flow for star 2 at several Wi .

V. FINAL REMARKS

The relatively good agreement of the MLD-R and GLaMM-R predictions with the experimental results has a significant implication: the response of entangled stars to startup shear can be described by simply manipulating an existing set of constitutive equations that apply to linear polymers. Because the shear rates explored in this study remained less than the inverse of the Rouse time, the effects of stretch have not been explored. However, it is not expected that the stretching dynamics would be changed qualitatively upon the introduction of a single branch point.

Our modeling suggests that at shear rates exceeding the longest relaxation time, CCR obviates deep arm fluctuations. Thus, CCR becomes the dominant relaxation mechanism and the GLaMM-R model’s detailed local implementation of CCR is more effective at describing our measurements. This also explains why, in the moderately non-linear flow regime ($\tau_d^{-1} \leq \dot{\gamma} \leq \tau_R^{-1}$), the transient response of star and linear polymers is very similar.

ACKNOWLEDGMENTS

This work was partially supported by the polymers program of the DMR at NSF and by the EPSRC through the Microscale Polymer Processing 2 project (Grant No. GR/T11807/01). The synthesis of the star polymers was carried out in the Polymer Synthesis

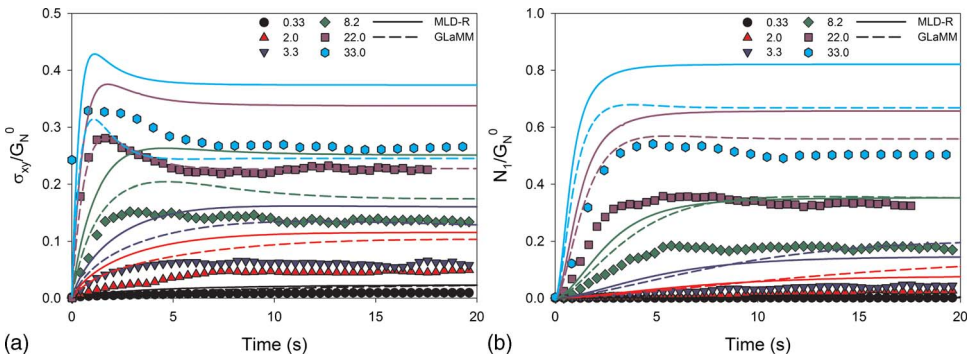


FIG. 14. (a) and (b) A comparison of MLD-R and GLaMM-R predictions with rheological data for startup of steady shear (derived from rheo-optical data) for star 2 at several Wi .

and Characterization Facility of the Materials Research Laboratory at UCSB, supervised by Dr. Krystyna Brzezinska. The collaboration between UCSB and Leeds University was initiated during the program on Complex Fluids at the ITP at UCSB (2002).

APPENDIX: THE THEORETICAL MODELS

1. The MLD-R model

The MLD model [Mead *et al.* (1996)] has been used to predict the transient behavior of entangled linear polymers subjected to the onset of shear flow. This model is based on the original Doi–Edwards model but has the added influences of chain stretch and CCR.

In a star molecule, the branch point strongly inhibits reptation. In applying the MLD model to stars, we approximate this by removing reptation altogether. The resulting code, which will be referred to as the MLD-R model, can be used to predict birefringence, orientation angle, shear stress, and first normal stress difference as a function of time for different shear rates.

The MLD model has been thoroughly described elsewhere in the original paper by Mead *et al.* (1998), as well as summarized in the Ph.D. thesis of Oberhauser (2001); however, its application to stars should be introduced in somewhat more detail. The basic idea is that the samples can be treated as two-arm stars with reptation disabled. The model will first be presented as applied to linear chains and then the adjustments that are needed to apply it to stars will be explained. A contour length variable s is introduced, as in the original MLD model, going from $-L/2$ at one end to $L/2$ at the other. s_0 is the curvilinear tube coordinate running along the relaxed tube, which has length L_0 . In the present use of the model, the tube length coordinate can be considered as running from $L/2$ at the free end and 0 at the center. So the actual implementation of the linear analysis looks at the behavior of only half of a chain and then doubles the quantities where necessary to give total stress, etc., for the full chain. Because of symmetry, the two approaches are equivalent. In the case of the star, each arm is considered independently; but by removing reptation and defining relaxation by CLFs to begin at the free end, rather than both ends, the constraints of the branch point are still described.

The equation for the tube survival probability function G depends on s , the present time t , and the past time t' . Past time represents the deformation history the material has experienced and could be understood as representing its memory,

$$\frac{\partial G(s,t,t')}{\partial t} = D \frac{\partial^2 G}{\partial s^2} - \langle v(s,t) \rangle \frac{\partial G}{\partial s} + f \left(\frac{\partial s}{\partial s_0} \right) \left[\frac{2}{L(t)} (s - \langle v(s,t) \rangle)_{s=L/2} \right] G - \frac{G}{\tau(s_0)}. \quad (\text{A1})$$

This equation for the tube survival probability function is based on the convection-diffusion equation from the Doi–Edwards model, but it has two additional terms. The third term on the right hand side accounts for the release of entanglements by relative chain motion, which makes up part of the CCR. The final term on the right hand side accounts for the effects of CLFs, as the repeated retractions of the arm into its tube allow segmental orientation to relax. This term depends on a relaxation time that is a function of the coordinate s_0 . The best description of CLFs uses a non-dimensionalized curvilinear coordinate x that has a value of 0 at the free end, when $s_0=L/2$, and a value of 1 at the center when s_0 is equal to 0. In using this coordinate transformation, it is straightforward to describe the fluctuations which become entropically unfavorable as they reach toward the center of the polymer, leading to the exponential dependence of the relaxation time $\tau(x)$, where x is defined as

$$x = 1 - 2 \left(\frac{s_0}{L_0} \right). \quad (\text{A2})$$

The relaxation time $\tau(x)$ depends on an effective potential,

$$\tau(x) = \sqrt{\frac{\pi^5}{6}} \tau_e Z^{3/2} \frac{e^{U_{\text{eff}}(x)}}{\left(x^2(1-x^2) + \frac{2}{3\pi Z} \right)^{1/2}}, \quad (\text{A3})$$

$$U_{\text{eff}}(x) = 3Z \left(\frac{x^2}{2} - \frac{x^3}{3} \right). \quad (\text{A4})$$

This formulation for the CLF relaxation times originates from the tube theory application to stars, whose primary orientational configuration renewal in the linear viscoelastic regime has been shown to be due to CLFs. This version has dynamic dilution already built-in, meaning that the chain ends are allowed to fluctuate while simultaneously the tube in which they are fluctuating is growing due to the release of entanglements by relaxed segments of neighboring chains. This form of the CLF component of the equation differs from the Doi–Kuzuu form used in the original MLD model and is instead based on the most recent and successful models for CLF coming from [Milner and McLeish \(1998\)](#), and with prefactors later corrected by [Likhman and McLeish \(2002\)](#).

The self-consistent switch function is used to the transition from tube shortening once the chain returns to its equilibrium length L_0 to tube reorientation; it simply preferentially applies CCR to chain stretch when it exists and ensures that the chain length is never decreased below its equilibrium length (except in the case of flow reversal),

$$f \left(\frac{\partial s}{\partial s_0} \right) = \left(\frac{\partial s}{\partial s_0} \right)^{-1}. \quad (\text{A5})$$

The curvilinear diffusion coefficient is used to account for reptation in the tube survival probability function and is defined as

$$D = \frac{L_0^2}{\tau_d \pi^2} = \frac{L_0^2}{3Z^3 \tau_e \pi^2}. \quad (\text{A6})$$

The tube survival probability function also depends on the ensemble average of the relative tube-chain velocity,

$$\langle v(s, t) \rangle = \kappa: \int_0^s \mathbf{S}(s', t) ds', \quad (\text{A7})$$

where κ is the velocity gradient tensor and \mathbf{S} is the orientation tensor,

$$\mathbf{S}(s, t) = \int_{-\infty}^t \frac{\partial G}{\partial t'} \mathbf{Q}(\mathbf{E}(t, t')) dt'. \quad (\text{A8})$$

The Doi–Edwards universal tensor is used without the independent alignment assumption

$$\mathbf{Q}(\mathbf{E}(t, t')) = \frac{1}{\langle \mathbf{E} \cdot \mathbf{u} \rangle_0} \left\langle \frac{(\mathbf{E} \cdot \mathbf{u})(\mathbf{E} \cdot \mathbf{u})}{|\mathbf{E} \cdot \mathbf{u}|} \right\rangle_0. \quad (\text{A9})$$

\mathbf{E} is defined as is customary: the deformation gradient tensor, and u is the unit vector distributed randomly over the unit sphere.

In order to apply these equations to stars, Eq. (A1) must be reconsidered,

$$\frac{\partial G(s,t,t')}{\partial t} = D \frac{\partial^2 G}{\partial s^2} - \langle v(s,t) \rangle \frac{\partial G}{\partial s} + f \left(\frac{\partial s}{\partial s_0} \right) \left[\frac{2}{L(t)} (\dot{s} - \langle v(s,t) \rangle)_{s=L/2} \right] G - \frac{G}{\tau(s_0)}. \quad (\text{A10})$$

In Eq. (A10), the first term on the right hand side is removed in order to discount any contributions from reptation to the tube survival probability function. This is done in a straightforward manner by the elimination of the term containing the diffusion coefficient D , which describes reptation. Physically, it becomes apparent that, while reptation is no longer present for stars, there should still be contributions from convection of the tube, CCR, and CLFs.

The MLD model allows CCR to contribute to both stretch relaxation and orientational relaxation, with the switch function leading to preferentially relaxed stretch. The stretch function $s(s_0, t)$ defines the change of the tube from its initial length, with s_0 being defined as the tube coordinate that runs along the relaxed tube. The equation governing the stretch function can be written in the form

$$\frac{\partial s}{\partial t} = \langle v(s,t) \rangle + \frac{L_0^2}{\tau_R \pi^2} \frac{\partial^2 s}{\partial s_0^2} - \frac{1}{2} \left[\frac{2}{L(t)} (\langle v(s,t) \rangle - \dot{s})_{s=L/2} \right] (s - s_0). \quad (\text{A11})$$

The first term on the right hand side accounts for the relative tube-chain velocity in the flow. The second term accounts for the chain retraction from the Rouse-based diffusivity and maintains a limited stretching for the chain. The third term on the right hand side allows for additional stretch relaxation through CCR.

The stress tensor is defined as

$$\sigma(t) = \frac{15}{4} G_N^0 \frac{2}{L_0} \int_0^{L/2} ds_0 \mathbf{S}(s_0, t) \left(\frac{\partial s}{\partial s_0} \right)^2. \quad (\text{A12})$$

The boundary and initial conditions are applied at the free ends and the chain centers,

$$G(s,t,t') = 0 \text{ at } s = L/2; \quad \frac{\partial G}{\partial s_0} = 0; \text{ at } s = 0; \quad G(s,t,t') = 1 \text{ at } t = t', \quad (\text{A13})$$

$$\frac{\partial s(s_0, t)}{\partial s_0} = 1 \text{ at } s = L/2; \quad s = 0 \text{ at } s_0 = 0; \quad \frac{\partial s(s_0, t)}{\partial s_0} = 1 \text{ at } t = 0. \quad (\text{A14})$$

This set of equations defines the stress response of entangled linear polymers to different flows and has been adapted in order to do the same for entangled star polymers. In order to determine the necessary parameters needed to model star behavior, the number of entanglements is taken as the number of entanglements per arm. Each arm relaxes only by CLF and CCR when reptation is disabled. Relaxation by CLF occurs for each arm independently so the entanglements of each half of the two-arm span are independent of one another, just as is physically the case in the star. In the numerical simulations of the transient response, the partial differential equations are solved using a Crank–Nicholson algorithm and the integral equations are computed using the trapezoid rule.

2. The GLaMM-R model

The GLaMM model [Graham *et al.* (2003)] is established as a reliable predictor of the nonlinear rheology of monodisperse linear polymer melts. In this model, the relaxation mechanisms of reptation, CLFs, retraction, and CR are formulated into a stochastic microscopic evolution equation for the dynamics of a space-curve describing the tube con-

tour $\mathbf{R}(s, t)$ where s is a continuous variable labeling the distance along the tube contour and t is time. From this equation, a deterministic partial differential equation for the tube tangent vector correlation function,

$$f_{\alpha\beta}(s, s'; t) \equiv \left\langle \frac{\partial R_{\alpha}(s, t)}{\partial s} \frac{\partial R_{\beta}(s', t)}{\partial s'} \right\rangle, \quad (\text{A15})$$

is derived. The resulting PDE is

$$\begin{aligned} \frac{\partial}{\partial t} f_{\alpha\beta}(s, s'; t) = & \kappa_{\alpha\gamma} f_{\gamma\beta} + f_{\alpha\gamma} \kappa_{\gamma\beta} + \frac{1}{3\pi^2 Z \tau_e} \left(\frac{Z}{Z^*(t)} \right)^2 \left(\frac{\partial}{\partial s} + \frac{\partial}{\partial s'} \right) \frac{D^*(s, s')}{\lambda(s, s')} \left(\frac{\partial}{\partial s} + \frac{\partial}{\partial s'} \right) f_{\alpha\beta} \\ & + \frac{3a\nu}{2} \left[\frac{\partial}{\partial s} \frac{1}{\lambda(s)} \frac{\partial}{\partial s} (f_{\alpha\beta} - f_{\alpha\beta}^{eq}) + \frac{\partial}{\partial s'} \frac{1}{\lambda(s')} \frac{\partial}{\partial s'} (f_{\alpha\beta} - f_{\alpha\beta}^{eq}) \right] \\ & + \frac{R_s}{2\pi^2 \tau_e} \left[\frac{\partial}{\partial s} \left(f_{\alpha\beta} \frac{\partial}{\partial s} \ln \lambda^2(s) \right) + \frac{\partial}{\partial s'} \left(f_{\alpha\beta} \frac{\partial}{\partial s'} \ln \lambda^2(s') \right) \right], \end{aligned} \quad (\text{A16})$$

where the first term describes the advection by the flow, and the second contains both reptation and CLF [from the effective local diffusion constant $D^*(s, s')$]. Here Z is the equilibrium number of entanglement segments comprising the chain and $Z^*(t)$ is the time-dependent instantaneous value that may differ from Z because of the chain stretch. The third term arises from CR and models the *tube* as a free polymer-like object with a local hopping rate ν . Here a is the “tube diameter” and $\lambda(s)$ is the local mean stretch of the chains given by $\lambda(s) = \sqrt{\text{Tr} f_{\alpha\beta}(s, s')}$. The CR rate ν is calculated self-consistently from averages of both thermal diffusion and retraction (CCR). Here, as elsewhere, we take $c_\nu = 0.1$ for the CR parameter. For full details, see [Graham *et al.* \(2003\)](#).

To extend this model to star polymers, we make a simple modification of the effective local diffusion constant $D^*(s, s')$. For linear polymers, this represents the crossover from CLFs to reptation dynamics and is written as

$$D^*(s, s') = \begin{cases} \frac{1.15^2}{s_{\min}^2} & s_{\min} < 1.15\sqrt{Z} \\ \frac{1}{Z} & \text{otherwise,} \end{cases} \quad (\text{A17})$$

where s_{\min} is the shortest distance of s or s' from either end of the chain. For stars reptation is suppressed so we set the $1/Z$ term to zero, which is the only change made.

References

- Auhl, D., J. Ramirez, A. E. Likhtman, P. Chambon, and C. Fernyhough, “Linear and nonlinear shear flow behavior of monodisperse polyisoprene melts with a large range of molecular weights,” *J. Rheol.* **52**, 801–835 (2008).
- Bero, C. A., and C. M. Roland, “Terminal relaxations in linear and three-arm star polyisoprenes,” *Macromolecules* **29**, 1562–1568 (1996).
- Bhattacharjee, P. K., J. P. Oberhauser, G. H. McKinley, L. G. Leal, and T. Sridhar, “Extensional rheometry of entangled solutions,” *Macromolecules* **35**, 10131–10148 (2002).
- Brown, E. F., W. R. Burghardt, H. Kahvand, and D. C. Venerus, “Comparison of optical and mechanical measurements of second normal stress difference relaxation following step strain,” *Rheol. Acta* **34**, 221–234 (1995).

- Chai, C. K., J. Creissel, and H. Randrianantoandro, "Flow-induced birefringence of linear and long chain-branched metallocene polyethylene melts subject to steady start-up flow," *Polymer* **40**, 4431–4436 (1999).
- Chow, A. W., and G. G. Fuller, "Response of moderately concentrated xanthan gum solutions to time-dependent flows using two-color flow birefringence," *J. Rheol.* **28**, 23–43 (1984).
- Fetters, L. J., A. D. Kiss, D. S. Pearson, G. F. Quack, and F. J. Vitus, "Rheological behavior of star-shaped polymers," *Macromolecules* **26**, 647–654 (1993).
- Geffroy, E., and L. G. Leal, "Flow birefringence studies in transient flows of a two roll mill for the test fluid M1," *J. Non-Newtonian Fluid Mech.* **35**, 361–400 (1990).
- Geffroy, E., and L. G. Leal, "Flow birefringence studies of a concentrated polystyrene solution in a two-roll mill. I. Steady flow and start-up of steady flow," *J. Polym. Sci., Part B: Polym. Phys.* **30**, 1329–1349 (1992).
- Graham, R. S., A. E. Likhtman, T. C. B. McLeish, and S. T. Milner, "Microscopic theory of linear, entangled polymer chains under rapid deformation including chain stretch and convective constraint release," *J. Rheol.* **47**, 1171–1200 (2003).
- Inoue, T., Y. Yamashita, and H. Watanabe, "Stress overshoot of entangled polymers in theta solvent," *Macromolecules* **37**, 4317–4320 (2004).
- Isaki, T., "Biaxial damping function of entangled monodisperse polystyrene melts: Comparison with the Mead–Larson–Doi model," *J. Rheol.* **47**, 1201–1210 (2003).
- Islam, M. T., and L. A. Archer, "Nonlinear rheology of highly entangled polymer solutions in start-up and steady shear flow," *J. Polym. Sci., Part B: Polym. Phys.* **39**, 2275–2289 (2001).
- Likhtman, A. E., and T. C. B. McLeish, "Quantitative theory for linear dynamics of linear entangled polymers," *Macromolecules* **35**, 6332–6343 (2002).
- Macosko, C. W., *Rheology: Principles, Measurements, and Applications* (Wiley-VCH, New York, 1994).
- McLeish, T. C. B., "Tube theory of entangled polymer dynamics," *Adv. Phys.* **51**, 1379–1527 (2002).
- Mead, D. W., R. G. Larson, and M. Doi, "A molecular theory for fast flows of entangled polymers," *Macromolecules* **31**, 7895–7914 (1998).
- Menezes, E. V., and W. W. Graessley, "Nonlinear rheological behavior of polymer systems for several shear-flow histories," *J. Polym. Sci., Polym. Phys. Ed.* **20**, 1817–1833 (1982).
- Milner, S. T., and T. C. B. McLeish, "Parameter-free theory for stress relaxation in star polymer melts," *Macromolecules* **30**, 2159–2166 (1997).
- Milner, S. T., and T. C. B. McLeish, "Reptation and contour-length fluctuations in melts of linear polymers," *Phys. Rev. Lett.* **81**, 725–728 (1998).
- Milner, S. T., T. C. B. McLeish, and A. E. Likhtman, "Microscopic theory of convective constraint release," *J. Rheol.* **45**, 539–563 (2001).
- Oberhauser, J. P., "Experimental and theoretical studies of the dynamics of entangled polymer solutions in time dependent shear flows" Ph.D. thesis, University of California, 2001.
- Oberhauser, J. P., L. G. Leal, and D. W. Mead, "The response of entangled polymer solutions to step changes of shear rate: Signatures of segmental stretch," *J. Polym. Sci., Part B: Polym. Phys.* **36**, 265–280 (1998).
- Pattamaprom, C., and R. G. Larson, "Constraint release effects in monodisperse and bidisperse polystyrenes in fast transient shearing flows," *Macromolecules* **34**, 5229–5237 (2001).
- Pearson, D. S., A. D. Kiss, L. J. Fetters, and M. Doi, "Flow-induced birefringence of concentrated polystyrene solutions," *J. Rheol.* **33**, 517–535 (1989).
- Raju, V. R., E. V. Menezes, G. Marin, and W. W. Graessley, "Concentration and molecular weight dependence of viscoelastic properties in linear and star polymers," *Macromolecules* **14**, 1668–1676 (1981).
- Sanchez-Reyes, J., and L. A. Archer, "Relaxation dynamics of entangled polymer liquids in steady shear flow," *J. Rheol.* **47**, 469–482 (2003).
- Schweizer, T., J. van Meerveld, and H. C. Ottinger, "Nonlinear shear rheology of polystyrene melt with narrow molecular weight distribution—Experiment and theory," *J. Rheol.* **48**, 1345–1363 (2004).
- Shull, K. R., E. J. Kramer, and L. J. Fetters, "Effect of number of arms on diffusion of star polymers," *Nature (London)* **345**, 790–791 (1990).
- Tezel, A. K., "Nonlinear rheology of entangled symmetric and asymmetric star polymers," Ph.D. thesis, University of California, 2005.

- Tezel, A. K., L. G. Leal, and T. C. B. McLeish, "Rheo-optical evidence for the existence of CCR in an entangled, monodisperse 4-arm star," *Macromolecules* **38**, 1451–1455 (2005).
- Vega, D. A., and S. T. Milner, "Shear damping function measurements for branched polymers," *J. Polym. Sci., Part B: Polym. Phys.* **45**, 3117–3136 (2007).
- Watanabe, H., S. Ishida, and Y. Matsumiya, "Rheodielectric behavior of entangled cis-polyisoprene under fast shear," *Macromolecules* **35**, 8802–8818 (2002).
- Ye, X., R. G. Larson, C. Pattamaprom, and T. Sridhar, "Extensional properties of monodisperse and bidisperse polystyrene solutions," *J. Rheol.* **47**, 443–468 (2003).
- Ye, X., and T. Sridhar, "Shear and extensional properties of three-arm polystyrene solutions," *Macromolecules* **34**, 8270–8277 (2001).